A Composition-Dependent Model for the Complex Dielectric Function of $\mathbf{In_{1-x}Ga_xAs_yP_{1-y}}$ Lattice-Matched to InP.*

Leonard I. Kamlet and Fred L. Terry, Jr.

Department of Electrical Engineering & Computer Science

111 DTM Bldg., The University of Michigan, 2360 Bonisteel Blvd., Ann Arbor, MI 48109-2108

Abstract

Accurate and numerically efficient models for the complex dielectric function versus wavelength and material characteristics are essential for the use of nondestructive optical techniques such as spectroscopic ellipsometry or reflectometry. These optical techniques are commonly used for real-time and run-to-run monitoring and control of growth and etch processes to determine a material's composition and thickness.

In this work, we discuss an improved composition-dependent model for the complex dielectric function for lattice-matched $In_{1-x}Ga_xAs_yP_{1-y}$/InP systems valid over the entire composition range $0 \leq y \leq 1$. We describe our model, which is an extension of the critical point parabolic band method and is based on the model proposed by Charles Kim et. al. for the $Al_xGa_{1-x}As$/GaAs system. We demonstrate the quality of the model in fitting optical data for individual compositions, and compare our results to other established models including the harmonic oscillator approximation and the model of Adachi. Using results obtained from the individual fits, we generate a composition-dependent model that is valid for the entire range of lattice-matched compositions. Also, we show how this model can be used to accurately determine the composition ($\pm$ 0.01) of an unknown material whose dielectric response has been obtained using spectroscopic ellipsometry or a similar technique.

*This material is based on work supported under a National Science Foundation Graduate Fellowship.

1 Introduction

Optical reflection measurement techniques such as spectroscopic ellipsometry[1–3] and reflectometry[4] are powerful methods for accurately determining the thicknesses of optically thin films. In most cases these methods are completely nondestructive and are, therefore, very useful for both in-situ and ex-situ monitoring for run-to-run control (process optimization), statistical quality control, and real-time control. For compound materials systems for which the dielectric functions are accurately known or modeled as functions of composition, these spectroscopic optical techniques can be used to accurately determine both layer thicknesses and compositions. However, errors in the model for a layer's dielectric response can lead to significant errors in the thin film thickness. For analysis of compound materials, a model which faithfully reproduces the dielectric response at known compositions and accurately interpolates between these compositions is critical. For use in control applications, this model must also be numerically efficient enough to permit its use in regression algorithms on relatively inexpensive computer workstations.

According to single electron theory, direct interband transitions around high-symmetry regions in the band structure (critical points) dominate the basic structure of the optical dielectric response for most semiconductor materials[5]. This theoretical approach neglects the effects of collective (many-body) interactions such as excitons, and ab initio calculations based on single electron theory will not accurately reproduce the dielectric function of a material (see for example [6]). On the other hand, an accurate first-principles model incorporating all many-body effects would be extremely impractical (if not impossible) to implement, and we expect that including a limited number of such many-body effects would result in modifications of the dielectric response near the critical points. Therefore, a phenomenological model which makes use of single electron theory around

critical points but which employs empirically adjustable parameters to incorporate the effects of collective interactions is attractive for optical reflection measurement applications. Also, since critical point energies are a strong function of a material's composition [7, 8, and references therein], this approach is favored over an empirical model such as the harmonic oscillator approximation which has no direct relation to the band structure.

In this paper, we will describe an improved phenomenological modeling procedure for the dielectric functions of lattice-matched compound semiconductors and will illustrate its use for the InGaAsP/InP system. $In_{1-x}Ga_xAs_yP_{1-y}$ lattice-matched to InP is an important materials system for optoelectronic devices such as lasers and photodetectors [9, and references therein] and is one of the relatively few compound semiconductor systems which have been characterized over their full compositional range. The model presented in this work is an extension of the work of Kim, et. al.[10–12] which employs estimates for the contributions to the dielectric function resulting from critical point transitions. We will present a fundamental improvement to Kim's model (the use of a harmonic oscillator baseline function which allows the entire dielectric response model to be Kramers-Kronig self-consistent), illustrate its use on the InGaAsP/InP alloy system, and show potential pitfalls in the application of the modeling procedure and how to avoid them.

The model is designed to describe all lattice-matched compositions over the entire range $0 \leq y \leq 1$. For each value of y, there is one value for x for which the quaternary $In_{1-x}Ga_xAs_yP_{1-y}$ is lattice-matched to InP. From Vegard's law this composition $x = \frac{.1896y}{.4176-.0125y}$[8].

In this work, we discuss our model and the theory behind it, using the same notation as in Kim's work for consistency. To create the composition-dependent model, we begin by individually fitting a number of compositions to published data. We first fit the compositional end points y=1 ($In_{0.53}Ga_{0.47}As$) and y=0 (InP), followed by fits to some intermediate compositions. We used data

from Aspnes and Stocker[13] for $In_{0.53}Ga_{0.47}As$, and data reported by Kelso, Aspnes, et. al.[9] for all other compositions. The data used for each fitting ranges from 1.5 to 6.0 eV.

We compare the quality of our individual fits to other established models including the model of Adachi and the harmonic oscillator approximation. The strengths and weaknesses of the methods will be discussed. Also, some of the critical point energies calculated during the fitting will be compared to published data.

Using results obtained from the individual fits, we generate a composition-dependent model that is valid for the entire range of lattice-matched compositions. Finally, we show how this model can be used to accurately determine the composition (± 0.01) of an unknown material whose dielectric response has been obtained using spectroscopic ellipsometry or a similar technique. This is demonstrated by fitting it to data for some lattice-matched samples with known compositions.

2 Modeling of dielectric function for unstrained semiconductors:

The model developed for optically isotropic semiconductors is based on a model proposed by Charles Kim[10, 11], and is based on the physical processes occurring in the semiconductor. The beginning of this discussion summarizes the theory behind Kim's model. Beginning with the formalism given by Ehrenreich and Cohen[14], the dielectric function without linewidth broadening is found to be

$$\epsilon(\omega) = 1 - \lim_{\eta \to 0} \frac{8\pi\hbar^2 e^2}{m^2} \sum_{c,v} \int dE' \frac{P_{cv}^2(E') J_{cv}(E')}{E'^2} \times \left[\frac{1}{\hbar\omega - E' + i\eta} - \frac{1}{\hbar\omega + E' + i\eta} \right] \quad (1)$$

where P_{cv}(E') is the momentum operator P_{cv}(**k**) averaged over a constant energy surface in

k - space and J_{cv}(E') is the joint density of states (JDOS) between the conduction and valence band states. P_{cv}(E') is a slowly-varying function of energy, and in this model it is treated as a quadratic polynomial using a power series expansion. For an unstrained semiconductor with a diamond or zinc-blende lattice structure, each optical transition can be described using either a three-dimensional JDOS or a combination of a two- and three-dimensional JDOS, using a parabolic-band approximation for energies near the critical points.

With broadening, η is replaced with a time-dependent function $\gamma(s)$ and we write the dielectric response as

$$\begin{aligned} \epsilon(\omega) &= 1 + i\frac{8\pi\hbar^2 e^2}{m^2}\sum_{c,v}\int dE' \frac{P_{cv}^2(E')J_{cv}(E')}{E'^2} \\ &\quad \times \left[\int_0^\infty ds\, e^{i[\hbar\omega - E' + i\gamma(s)]s} - \int_0^\infty ds\, e^{i[\hbar\omega + E' + i\gamma(s)]s}\right]. \end{aligned} \tag{2}$$

If $\gamma(s)$ is a constant ($= \Gamma$), the broadening is Lorentzian, and the dielectric response reduces to the form of equation 1, with η replaced by Γ. This case is solvable analytically. If on the other hand $\gamma(s)$ is described by the relation $\gamma(s) = 2\sigma^2 s$, the broadening is Gaussian and the integral in equation 2 is not solvable analytically. As in Kim's work, we solved the integral assuming Lorentzian broadening to obtain an analytical function. Kim then replaced each broadening term Γ_j with a term $D_j = \Gamma_j\ e^{(-\alpha_j(E-E_j^2))}$ to simulate the effects of Gaussian broadening; we will comment on this in the next section.

The summation over the conduction and valence band transitions is dominated by and is approximately equal to a summation of dominant optical transitions occurring at the critical points in the band structure. With those assumptions, we write the model for the dielectric response as

$$\epsilon(\omega) = 1 - \left\{ \sum_{\substack{3-D\ M_0 \\ critical\ points}} \left[\sum_{n=0}^{2} (p_n H_n + q_n F_n) \right] + \sum_{\substack{3-D\ M_1\ \&\ 2-D\ M_0 \\ critical\ points}} \left[\sum_{n=0}^{2} (p_n G_n + q_n K_n) \right] + \sum_{\substack{3-D\ M_2 \\ critical\ points}} \left[\sum_{n=0}^{2} (p_n G_n + q_n H_n) \right] \right\} + baseline \quad (3)$$

where p_n and q_n are amplitude fitting parameters. These parameters define the low-order polynomials we use to describe the momentum matrix elements, absorb many of the other constants, and incorporate the effects of the collective interactions. The terms H_n, F_n, G_n, and K_n are the various integrals with different forms for the JDOS. The integrals are defined in a range between any two critical points E_i and E_f as:

$$H_n = \int_{E_i}^{E_f} dE \, \frac{\sqrt{E - E_i}}{E^{2-n}} \times \left[\Phi\left(\hbar\omega - E\right) - \Phi\left(\hbar\omega + E\right) \right] \quad (4a)$$

$$F_n = \int_{E_i}^{E_f} dE \, \frac{\sqrt{E - E_i}\sqrt{E_f - E}}{E^{2-n}} \times \left[\Phi\left(\hbar\omega - E\right) - \Phi\left(\hbar\omega + E\right) \right] \quad (4b)$$

$$G_n = \int_{E_i}^{E_f} dE \, \frac{1}{E^{2-n}} \times \left[\Phi\left(\hbar\omega - E\right) - \Phi\left(\hbar\omega + E\right) \right] \quad (4c)$$

$$K_n = \int_{E_i}^{E_f} dE \, \frac{\sqrt{E_f - E}}{E^{2-n}} \times \left[\Phi\left(\hbar\omega - E\right) - \Phi\left(\hbar\omega + E\right) \right], \quad (4d)$$

where

[1] It should be noted here that the equation Kim provides for F_2[10, Appendix A, eq. A.15] has a sign error. The second fraction should be subtracted from the first, not added to it.

$$\Phi\left(\hbar\omega \pm E\right) \equiv \frac{1}{\hbar\omega \pm E + i\Gamma(E)}, \tag{5a}$$

with

$$\Gamma(E) \equiv \gamma E + \beta \tag{5b}$$

$$\gamma \equiv \frac{\Gamma_f - \Gamma_i}{E_f - E_i} \tag{5c}$$

$$\beta \equiv \frac{E_f\Gamma_i - E_i\Gamma_f}{E_f - E_i} \tag{5d}$$

After the integration, the Γ_i and Γ_f are replaced by the Gaussian-corrected broadening terms described above. So for each critical point, we can fit up to nine parameters: six amplitude parameters (p_0, p_1, p_2, q_0, q_1, and q_2), the critical point energy and linewidth, and the broadening correction term α.

One difference between this model and the one described by Kim, which is subtle but important, is the form of the baseline equation used in the model. A baseline function must be included in this model to account for transitions above the highest energy in the measured data. But Kim's use of a quadratic polynomial as the baseline function has two problems. First, such an equation is not properly weighted to the higher energies as it should be. Second, and more importantly, such a generic polynomial does not satisfy the Kramers-Kronig relation, which requires the real part of the dielectric response to be an even function and the imaginary part to be an odd function. In this work we have chosen to use a Lorentzian baseline of the form

$$Ae^{i\phi}\left(\frac{1}{\hbar\omega - E_c + i\Gamma} - \frac{1}{\hbar\omega + E_c + i\Gamma}\right). \tag{6}$$

This choice of baseline is Kramers-Kronig consistent[15] and is centered about a higher energy E_c, chosen to be 6.5 eV in this work since our data only goes up to 6.0 eV. We also fix $\Gamma = 0.1$, so

only two parameters for the baseline equation are fitted in this work.

2.1 Procedure

To generate the composition-dependent model for the dielectric function, we first apply the model described above to individual lattice-matched compositions of $In_{1-x}Ga_xAs_yP_{1-y}$ for which dielectric response data is available. The Levenberg-Marquardt[16, 17] nonlinear regression method was used to perform the fitting.

Seven critical points were used in each of the individual fits. These corresponded to optical transitions at the critical points identified (in order of increasing energy) as $E_0(\Gamma)$, $E_0 + \Delta_0$, $E_1(L)$, $E_1 + \Delta_1$, $E_2(X)$, $E_0^{'}(\Delta)$, and $E_2(K)$. It should be pointed out that for this material system, the E_0 and $E_0 + \Delta_0$ critical points are below the range of measured data, which begins at 1.5 eV. They do affect the dielectric function below the E_1 transition, however, and therefore must be included in the model even though it becomes more difficult to confirm whether the fitted values are correct.

As stated above, for each critical point there are up to nine parameters that may be fitted; for this work we allowed all the parameters except α (the Gaussian/Lorentzian broadening correction factor) to vary. When we set all of the α terms to zero (assuming Lorentzian broadening), we obtained good fits to our data. When we allowed some of these corrective terms to be nonzero (on the order of 1) for the lower-energy critical points, we found that the individual fits improved slightly, especially near the critical point energies. In addition to the improvement in individual fits, the composition-dependent model was more accurate when we included the α terms. Since we are concerned about the accuracy of our composition-dependent model, we chose to include these terms, but we held them constant during the fitting. To choose the values of these parameters, we modified but did not

formally fit these terms until we saw an improvement in the individual fit for one composition, and then held those values constant for all other compositions.

For the baseline function, we allowed two parameters to vary (magnitude and phase), so we fit 58 parameters. Note that this is more than Kim used in his fitting, since he set many of his polynomial factors to zero in his work. We found no good method for selecting *a priori* which factors could be ignored for fitting a particular data set, so we chose to fit all of them for method generality.

After generating the individual fits, we use the critical point energies and linewidths from those fits to compute best-fit polynomial composition-dependent equations. Various authors[8, 18] have obtained good results using a quadratic fit to the critical point energies, so we also use a quadratic polynomial for our energies. Once those polynomials are calculated, we perform a simultaneous fit to all of our individual data sets to obtain composition-dependent amplitude parameters and baseline parameters. The equations for these composition-dependent parameters are cubic polynomials.

3 Results

3.1 Individual Fits

To verify the model discussed above, we first discuss the individual fit to $In_{0.53}Ga_{0.47}As$, the $y = 1$ composition that is lattice-matched to InP, and discuss solutions to potential pitfalls when using the model. We then show fits by the model to data for the dielectric response of InP, and a number of other $In_{1-x}Ga_xAs_yP_{1-y}$ compositions that are also lattice-matched to InP.

3.1.1 $In_{0.53}Ga_{0.47}As$

The results from our individual fit to $In_{0.53}Ga_{0.47}As$ is shown in Figure 1. We achieve an excellent fit to the data. The largest difference of any fitted value to its corresponding data point is 0.2 (ϵ/ϵ_0) for the ϵ_1 point at 6.0 eV (the end data point), and the average difference is $\sim$ 0.35 %.

When we first performed this fitting, we found differences between our critical-point energies and those reported in published data[8, 19]. Most authors have found E_0 to be between 0.71 and 0.75 eV, and $E_0 + \Delta_0$ to be between 1.04 and 1.10 eV. In our initial fit, we found E_0 = 0.65 eV and $E_0 + \Delta_0$ = 0.99 eV. These are both lower than expected. The E_1 value found (2.48 eV) was also slightly low, and the $E_1 + \Delta_1$ value (2.86 ± 0.01 eV) was acceptable, with published values typically near 2.83-2.84 eV.

Looking into the discrepancies, we noticed two potential problems with the model. First, it was possible to get a very good fit to the data and to first- and second-derivative spectra, while obtaining incorrect values for the critical-point energies. Also, it was possible to get a very good fit to the data but obtain amplitude parameters that cause the individual contributions to be physically incorrect. For example, we found that incorrect values for the amplitude polynomial terms for the E_0 and $E_0 + \Delta_0$ critical points can cause the contributions to the dielectric function due to these critical points to oscillate against each other. This would cause one of the two contributions to be non-physical ($\epsilon_2(\omega) < 0$), while making the net result match the shape of the low-energy part of the curve and minimize the χ^2 error. Since the upper bound in energy for these contributions to the dielectric response is E_1, this also tended to affect the value calculated for that energy.

This latter problem occurred only at lower energies, affecting the values calculated for E_0 and $E_0 + \Delta_0$. For this material system, these critical points fall below the range of energies for which

we have data. Also, there tends to be little structure in the data that is available above 1.5 eV, making precise fitting difficult. We believe that this problem is further magnified due to the number of parameters used in the fitting (eight for each critical point) and the close energy spacing between those critical points. By fitting fewer parameters, as Kim does for $Al_xGa_{1-x}As$ by setting some to zero and holding others constant, this problem may not be as much of an issue. We chose not to do this both because of the difficulty in selecting which parameters should be set to zero and because the additional parameters are useful for creating an accurate composition-dependent model. Still, we are able to resolve the critical point energies, although our amplitude parameters may lose some of their physical significance.

To investigate the first problem, we looked at the third-derivative JDOS spectra (= $E^{-2}\frac{\partial^3 E^2\epsilon}{\partial E^3}$), a common method for finding the critical points of a semiconductor. Specifically, the shape around the E_1 critical point is useful here in determining the appropriate choice of energies. Performing the fitting to the undifferentiated data again, we found more representative values for the true critical point energies. For this marked improvement in the energy determination, we achieved a barely noticeable improvement in the χ^2 error from the fit to the undifferentiated data. Figure 2-a shows the third-derivative JDOS spectra along with both the original fit and the improved fit, showing that the parameters found by the newer fit are better that those found originally. Figure 2-b shows the same fits to the undifferentiated data, showing that both provide high-quality fits to the data even though the original fit critical-point energies are incorrect.

In addition to suggesting that we must check our fits against the third-derivative JDOS, this result also makes an important statement concerning the quality of the data that is to be fitted. To look at a third-derivative spectra, the data collected must be of high quality so that noise is not a problem. The only sources of data widely available for this material system were produced by

Aspnes in the early 1980s, and he is currently working on collecting data from newer, higher quality samples[20]. We are reminded that the quality of any fit hinges directly on the accuracy and quality of the data being fit.

Of the other work modeling the dielectric function of $In_{0.53}Ga_{0.47}As$, the work by Sadao Adachi[8, 19, 21] is generally considered to be the most complete and most accurate. His model also starts out as a summation of critical point effects, but he accounts for the broadening terms differently, by calculating the integral without broadening and later adding a broadening term back into the equation. This likely leads to problems, and Adachi adds in other factors (e.g. contributions from indirect transitions) to account for discrepancies between his fits and the data. Others who use his models also tend to add extra terms in an effort to improve the fits. It is also important to point out that, for his fits to $In_{1-x}Ga_xAs_yP_{1-y}$ data[19], he does not fit the critical point energies, but rather uses energies published by others. Still, Adachi's published results for $In_{0.53}Ga_{0.47}As$ are less accurate than our results for the individual fit (see Figure 3).

The harmonic oscillator approximation (HOA)[22] can also be used with a good degree of accuracy in the fitting, but there is no physical relation between the energies obtained with the HOA method and the critical point energies in the material. The quality of fit from the HOA is comparable to the fit obtained from our model. Table 1 shows the energies for $In_{0.53}Ga_{0.47}As$ as given by this method, Adachi's work, and the HOA analysis. Adachi fits only five critical points for direct transitions, corresponding to the first five energies listed in the table, and the sixth energy entered is his value for an indirect energy transition that he also includes in his model. We see a good agreement between our energies and those of Adachi, and the HOA energies do not correspond to the critical point energies.

3.1.2 InP

Our fit to the dielectric function for InP is shown in Figure 4. The fit is excellent throughout the entire range of energies 1.5 $\leq$ E $\leq$ 6.0 eV. The largest difference of any fitted value to its corresponding data point is 0.054 (ϵ/ϵ_0) for the ϵ_1 point at 1.5 eV, and the average difference is $\sim$ 0.3 % for either ϵ_1 or ϵ_2.

In addition to the high quality of fit to the spectral data, the values we obtain for the critical point energies also agree well with numbers presented previously in the literature[8, pages 77, 81, and 83]. Our fit determined E_0 to be 1.33 $\pm$ 0.01 eV. This is in line with values found between 1.337 and 1.35 eV by various authors. Similarly, we found $E_0 + \Delta_0$ = 1.44 $\pm$ 0.01 eV, slightly below the literature values of 1.449 - 1.472 eV. Values found for E_1 (3.17 eV) and $E_1 + \Delta_1$ (3.25 eV) are also in good agreement with the published data. Table 2 shows critical point energies calculated from these methods.

As with the fit to $In_{0.53}Ga_{0.47}As$, the published fit of Adachi (figure 3) is not as good throughout the spectrum. Recently, Adachi has informed us[23] of achieving a better fit to the InP data than the fit that he has published, but the fit is still not quite as good throughout the entire data set. The HOA again provides a good fit but no information about the actual critical energies.

3.1.3 Other lattice-matched compositions of $\mathbf{In_{1-x}Ga_xAs_yP_{1-y}}$

In addition to the two compositional endpoints, data was available for lattice-matched compositions with y = 0.24, 0.42, 0.55, and 0.82. Shown in Figure 5 are fits to two of these intermediate compositions, with $y = 0.42$ and $y = 0.82$.

Problems fitting third-derivative JDOS spectra due to noise led to uncertainties in these critical-

point energy calculations. In many cases the best fit to the undifferentiated data was used without confirmation of the correct critical-point energy values. While not an ideal situation, this approach seemed to be acceptable for generating the composition-dependent model.

3.2 Composition-dependent model

Having calculated the critical point energies and linewidths and amplitude parameters for each of the materials individually, we now wish to use these results to develop a composition-dependent model. Again, we follow the basic procedure presented by Kim with some modifications.

First, we use the critical point energies and linewidths found individually to create composition-dependent polynomial fits. The general form for these equations is

$$E(y) = E(y=0) + [E(y=1) - E(y=0)]y + Ay(y-1) \quad (7)$$

$$\Gamma(y) = \Gamma(y=0) + [\Gamma(y=1) - \Gamma(y=0)]y + [A + By]y(y-1) \quad (8)$$

with A and B determined from the fitting. Kim used cubic equations to fit energies in his work with AlGaAs/GaAs, but as stated earlier other authors have found quadratic relations to be sufficient for describing the compositional dependence of the critical-point energies for this materials system. We reiterate here the importance of correctly solving for the critical-point energies when performing the individual fits. If the values found from the individual fits are incorrect, then the quadratic polynomials calculated here will be incorrect and the quality of the composition-dependent fit will suffer. Table 3 shows all of the energies obtained by the model described in this paper. In Figure 8 we show how our quadratic fit for E_0 compares to the findings of others[8, table 6.3, and references therein], showing that we do indeed obtain reasonable values for the critical point energies.

We then generate composition-dependent amplitude parameters as cubic polynomials by performing a simultaneous fit to all of the individual compositions, holding the energies and linewidth polynomial terms fixed. We now have 24 amplitude parameters for each critical point, plus eight parameters for the composition-dependent baseline, for a total of 176 parameters. Nevertheless, this fitting is fairly fast since only a few iterations are required. Also, we fit only the real part of the dielectric function to improve both the speed and accuracy of the composition-dependent model.

Fits resulting from this simultaneous fitting are shown in Figure 6. Three of the six compositions used are shown, corresponding to fits to $In_{0.53}Ga_{0.47}As$, $In_{0.81}Ga_{0.19}As_{0.42}P_{0.58}$, and InP. The fits to these data sets simultaneously are not as good as the individual fits, but this is to be expected since our model accounts for all lattice-matched compositions, for $0 \leq y \leq 1$.

This composition-dependent model has only a single unknown (y) for fitting unknown materials. To demonstrate the ability of this model to determine a material's composition, we supply our program with a set of data points from one of our known compositions, and ask the program to determine the correct composition. In Figure 7 we show two examples of these results. In the top graph, we supplied the program with data from the $y = 0.55$ data set, and the program concluded that its composition was 54 %. In the bottom graph, we supplied the program with data from the $y = 0.24$ data set, and in this case the program found 24 % to be the best fit. For all cases that we were able to run, the composition was determined to be accurate to ± 0.01.

4 Conclusions

We have demonstrated a composition-dependent model for fitting the dielectric function of $In_{1-x}Ga_xAs_yP_{1-y}$ lattice-matched to InP. The fitted values are generated quickly, taking less than 5 ms to generate the

real part of the dielectric response for a given composition and wavelength. Since the only inputs necessary are the composition and wavelength, the model data sets can be calculated either at run time or in advance when used in a lookup table. The model determines the composition of a sample to within 1 %.

We also described the procedure used to create the model, and pointed out the importance of calculating the critical-point energies correctly when performing the individual fits. We confirm the accuracy of these fitted energies by using third-derivative JDOS spectra. This implies that our data cannot have much noise, or else information in the third-derivative spectra may be obscured or lost.

References

[1] R. M. A. Azzam and N. M. Bashara, *Ellipsometry and Polarized Light* (Elsevier Publications, 1977).

[2] David E. Aspnes, in *Handbook of Optical Solids*(E. Palik, editor), pp. 89–112 (Academic Press, 1985).

[3] David E. Aspnes, *Characterization of semiconductors and semiconductor structures by photometric and ellipsometric techniques* (SPIE, 1987).

[4] O. S. Heavens, *Optical properties of thin solid films* (Dover, 1955).

[5] F. Bassani and G. Pastori Parravicini, *Electronic States and Optical Transitions in Solids* (Pergamon Press, 1975).

[6] J. A. van Vechten, *Phys. Rev.* **182**(3), 891 (1969).

[7] Jasprit Singh, *Physics of Semiconductors and Their Heterostructures* (McGraw-Hill, 1993).

[8] Sadao Adachi, *Physical Properties of III-V Semiconductor Compounds: InP, InAs,GaAs, GaP, InGaAs, and InGaAsP* (John Wiley and Sons, 1992).

[9] S. M. Kelso, D. E. Aspnes, M. A. Pollack, and R. E. Nahory, *Phys. Rev. B* **26**(12), 6669 (1982).

[10] Charles C. Kim, *New Model for the Dielectric Function of Semiconductors and the Improvement of Phase-Modulated Ellipsometry* (thesis, 1991).

[11] Charles C. Kim, James W. Garland, H. Abad, and Paul M. Raccah, *Phys. Rev. B* **45**(20), 11749 (1992).

[12] Charles C.and Garland Kim, James W., and Paul M. Raccah, *Phys. Rev. B* **47**(14), 1876 (1993).

[13] D. E. Aspnes and H. J. Stocker, *J. Vac. Sci. Technol.* **21**(2), 413 (1982).

[14] H. Ehrenreich and M. L. Cohen, *Phys. Rev.* **115**(4), 786 (1959).

[15] M. Erman, J. B. Theeten, N. Vodjdani, and Y. Demay, *J. Vac. Sci. Technol. B* **1**(2), 328 (1983).

[16] Donald W. Marquardt, *J. Soc. Indust. Appl. Math.* **11**(2), 431 (1963).

[17] W. H. Press, B. P. Flannery, S. A. Teukolsky, and W. T. Vetterling, *Numerical Recipes in C* (Cambridge University Press, 1988).

[18] Ernesto H. Perea, Emilio E. Mendez, and Clifton G. Fonstad, *Appl. Phys. Lett.* **36**(12), 978 (1980).

[19] Sadao Adachi, *Phys. Rev. B* **39**(17), 12612 (1989).

[20] David E. Aspnes, private communication.

[21] Sadao Adachi, *Phys. Rev. B* **35**(14), 7454 (1987).

[22] Fred L. Terry, Jr, *J. Appl. Phys.* **70**(1), 409 (1991).

[23] Sadao Adachi, private communication.

LIST OF TABLES

LIST OF FIGURES

(a): fit to the real part of the dielectric response.

(b): fit to the imaginary part of the dielectric response.

In both, symbols represent the data, and the lines correspond to the best fits.

Figure 6: Simultaneous fit to the real part of the dielectric functions of $In_{1-x}Ga_xAs_yP_{1-y}$ for $y = 1.0$ ($In_{0.53}Ga_{0.47}As$), $y = 0.42$, and $y = 0.0$ (InP).

The symbols represent the data, and the lines correspond to the best fits.

Figure 7: Best fits to data using the composition-dependent model.

(a) Best fit to the $y = 0.55$ composition. The model calculates that the composition of this sample is 54 %.

(b) Best fit to the $y = 0.24$ composition. The model calculates that the composition of this sample is 24 %.

In both, circles represent the data and the solid line is the best fit.

Figure 8: E_0 critical point energy as a function of composition.

Solid line with squares: results from this work. Long dashed line: results from Nahory, et. al. Short dashed line: results from Perea, et. al. Dotted line: results from Laufer, et. al.

Method	E_0	$E_0 + \Delta_0$	E_0	$E_1 + \Delta_1$	$E_2(X)$	E'_0	$E_2(K)$
Kamlet	0.75	1.04	2.57	2.83	4.41	4.52	4.70
Adachi	0.75	1.04	2.57	2.83	4.41	1.20	
HOA	2.63	2.73	3.93	4.51	4.61	4.76	6.23

Method	E_0	$E_0 + \Delta_0$	E_0	$E_1 + \Delta_1$	$E_2(X)$	E'_0	$E_2(K)$
Kamlet	1.33	1.44	3.17	3.25	4.40	4.82	4.99
Adachi	1.35	1.47	3.16	3.30	4.72	2.05	
HOA	3.00	3.13	4.12	4.77	4.89	5.04	6.32

% y	E_0	$E_0 + \Delta_0$	E_0	$E_1 + \Delta_1$	E_2(X)	E'_0	E_2(K)
0.00	1.330	1.440	3.170	3.250	4.400	4.820	4.990
0.24	1.154	1.319	2.931	3.124	4.461	4.684	4.819
0.42	1.037	1.239	2.791	3.040	4.482	4.608	4.733
0.55	0.962	1.185	2.712	2.985	4.485	4.568	4.693
0.82	0.826	1.089	2.602	2.885	4.456	4.522	4.670
1.00	0.752	1.035	2.571	2.831	4.411	4.520	4.700

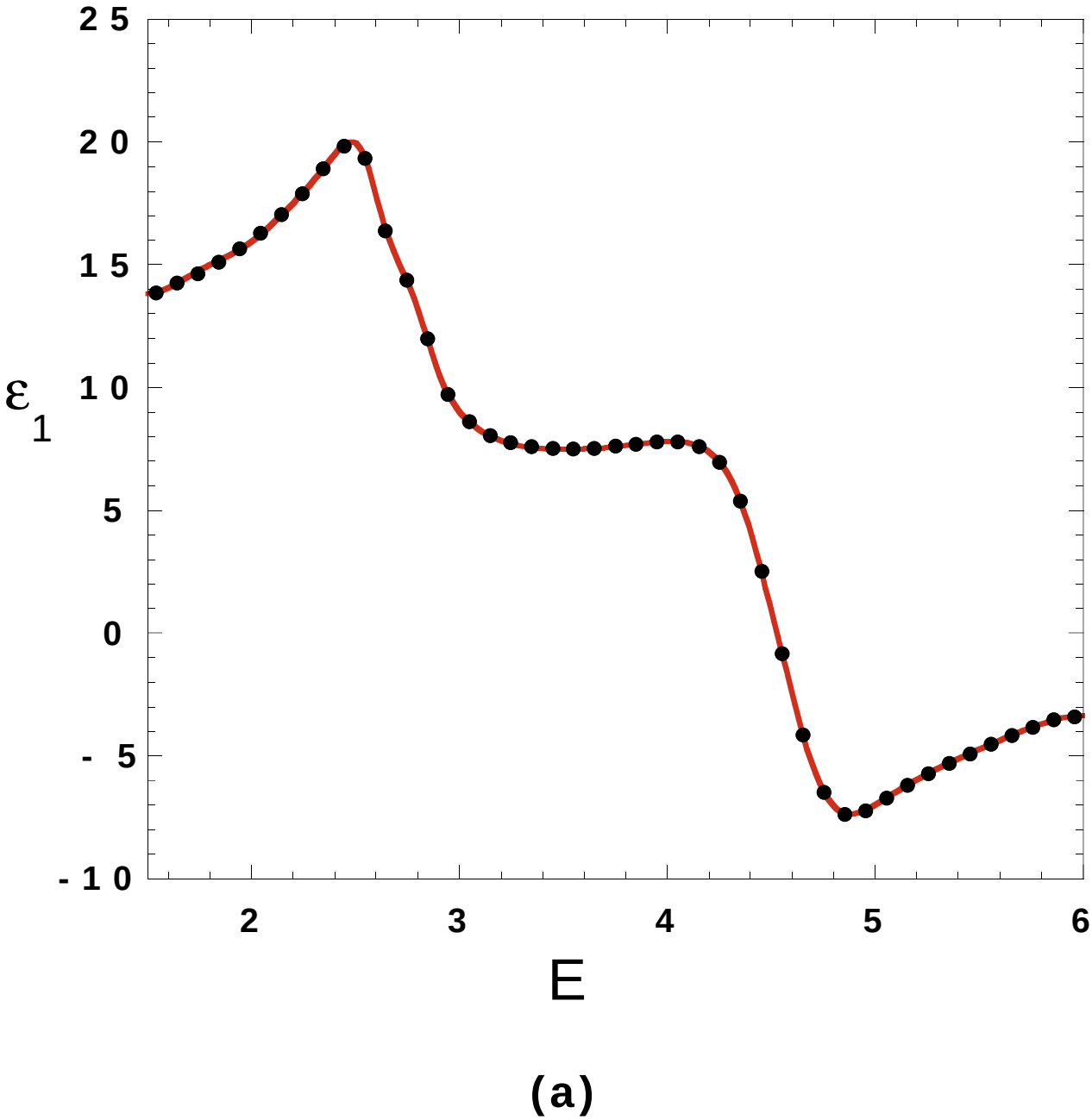

(a)

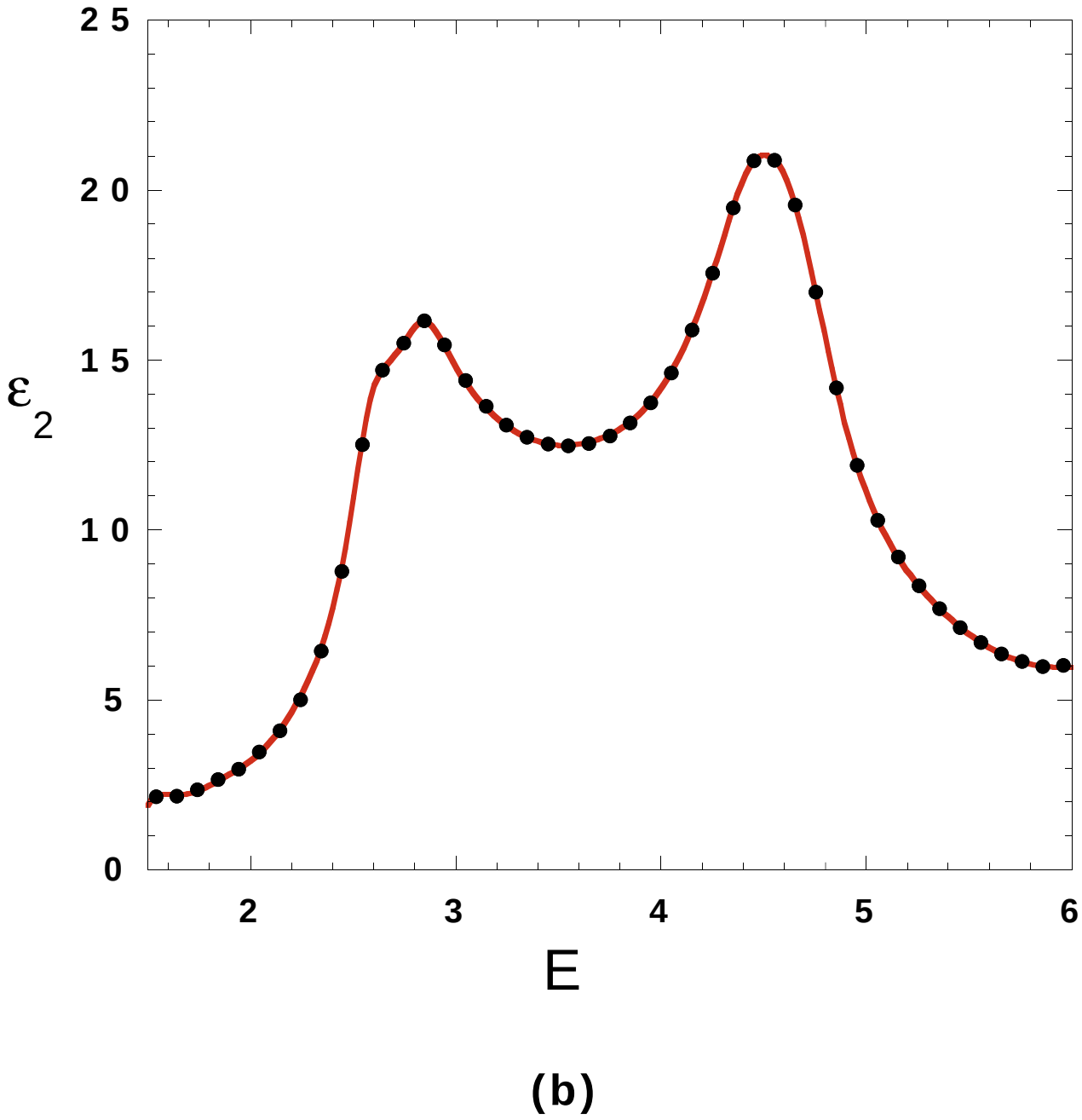

(b)

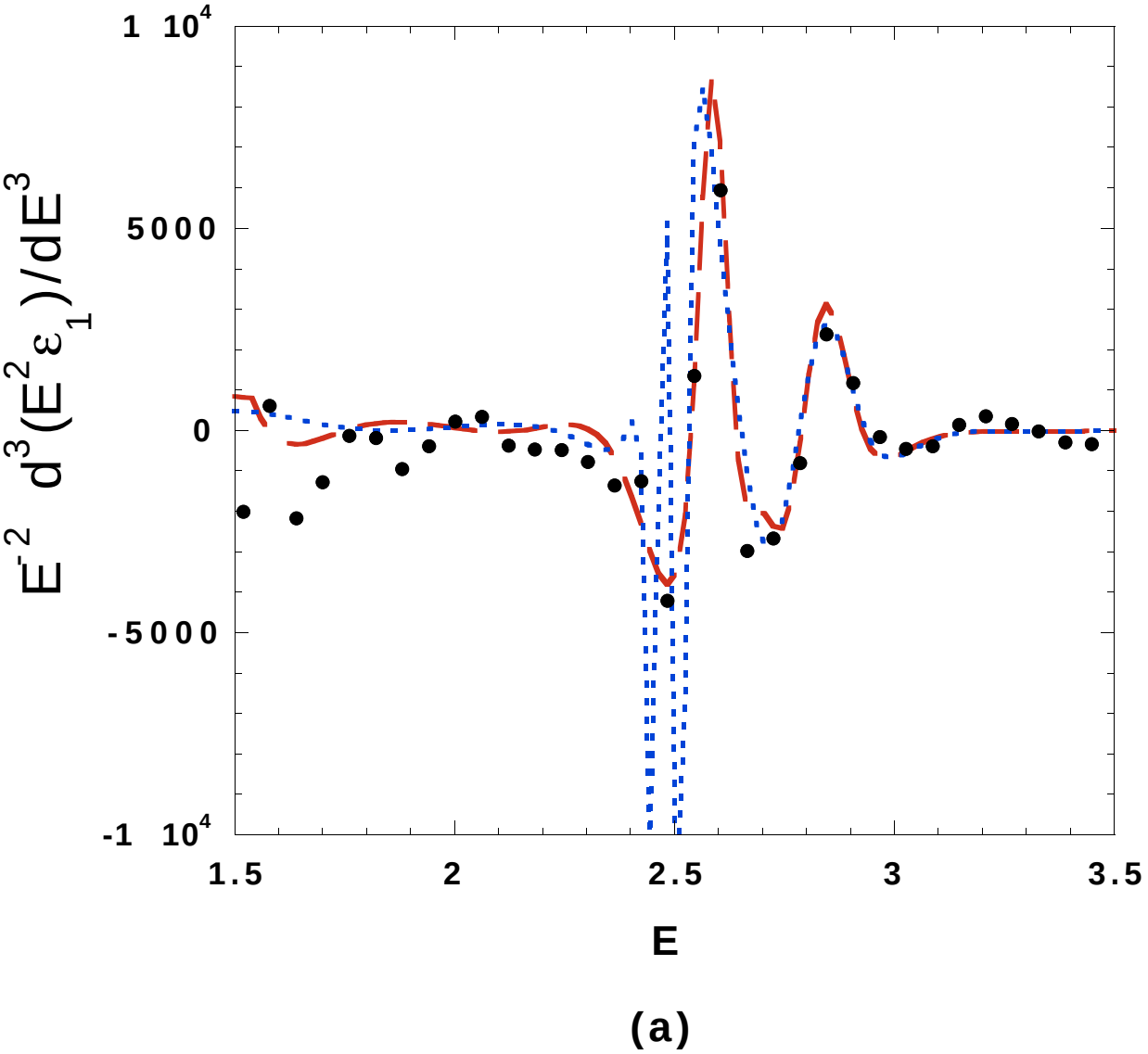

(a)

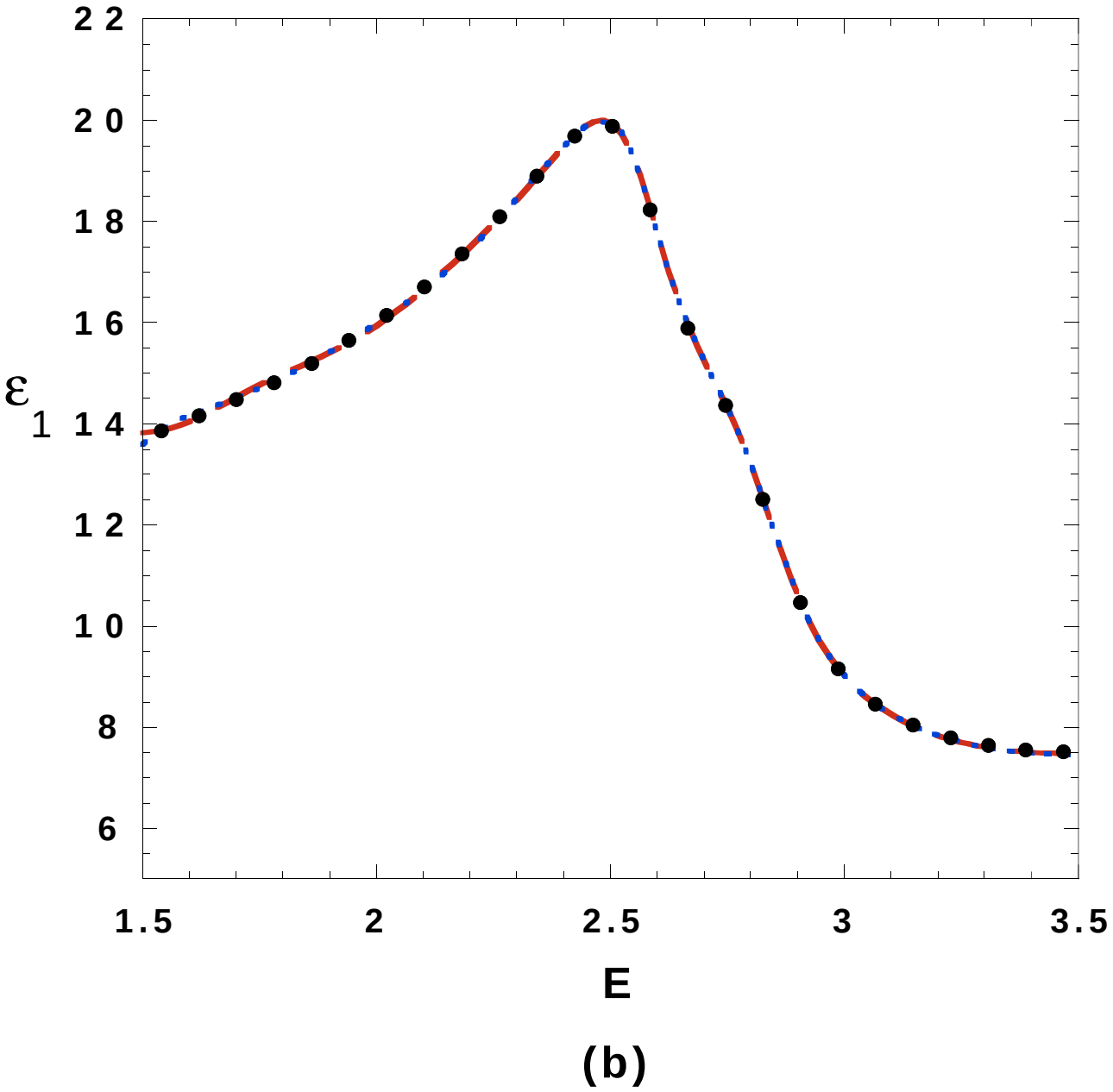

(b)

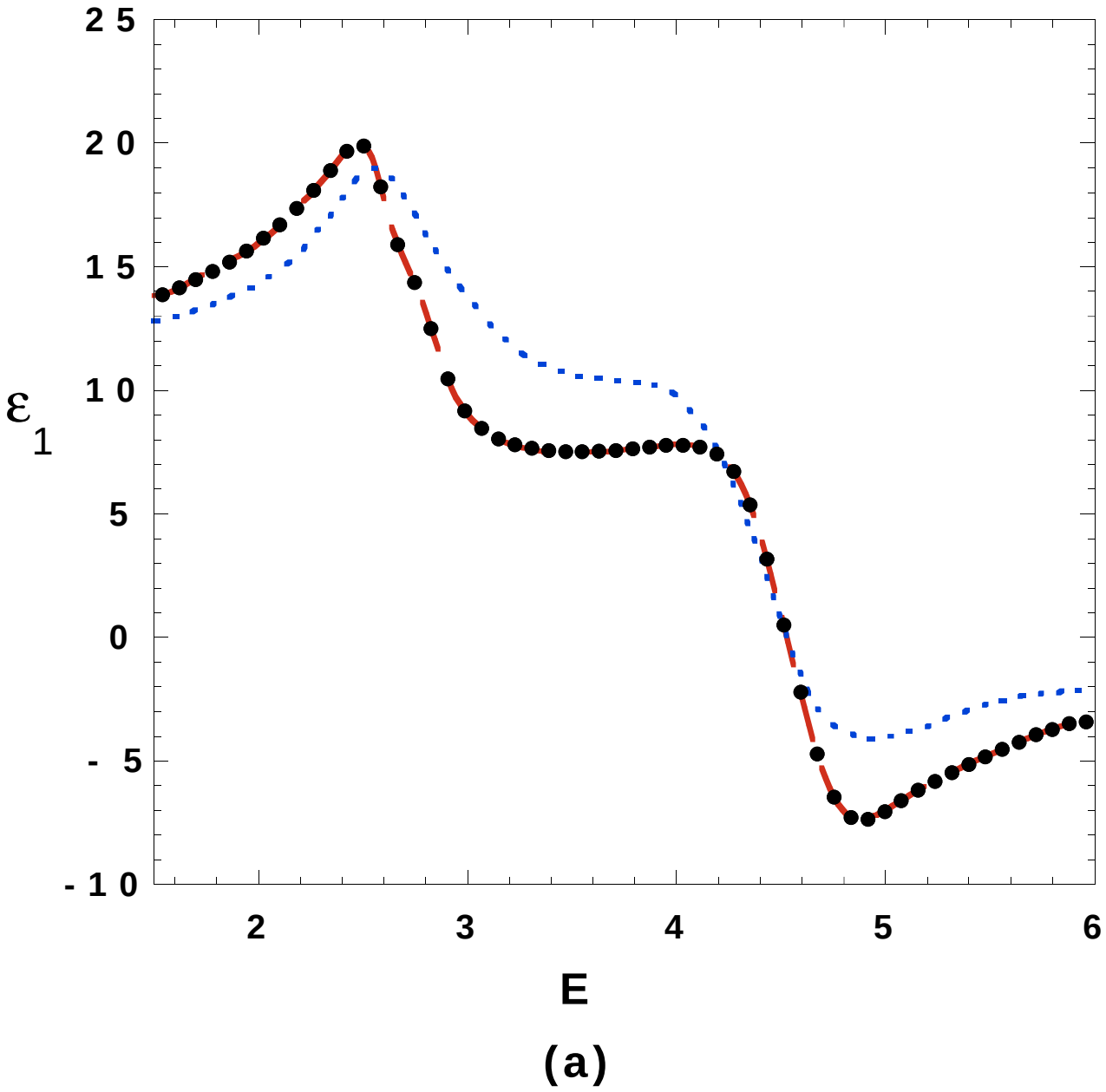
2 5
2 0
1 5
1 0
5
0
- 5
- 1 0
ε1
2
3
4
5
6
E
(a)

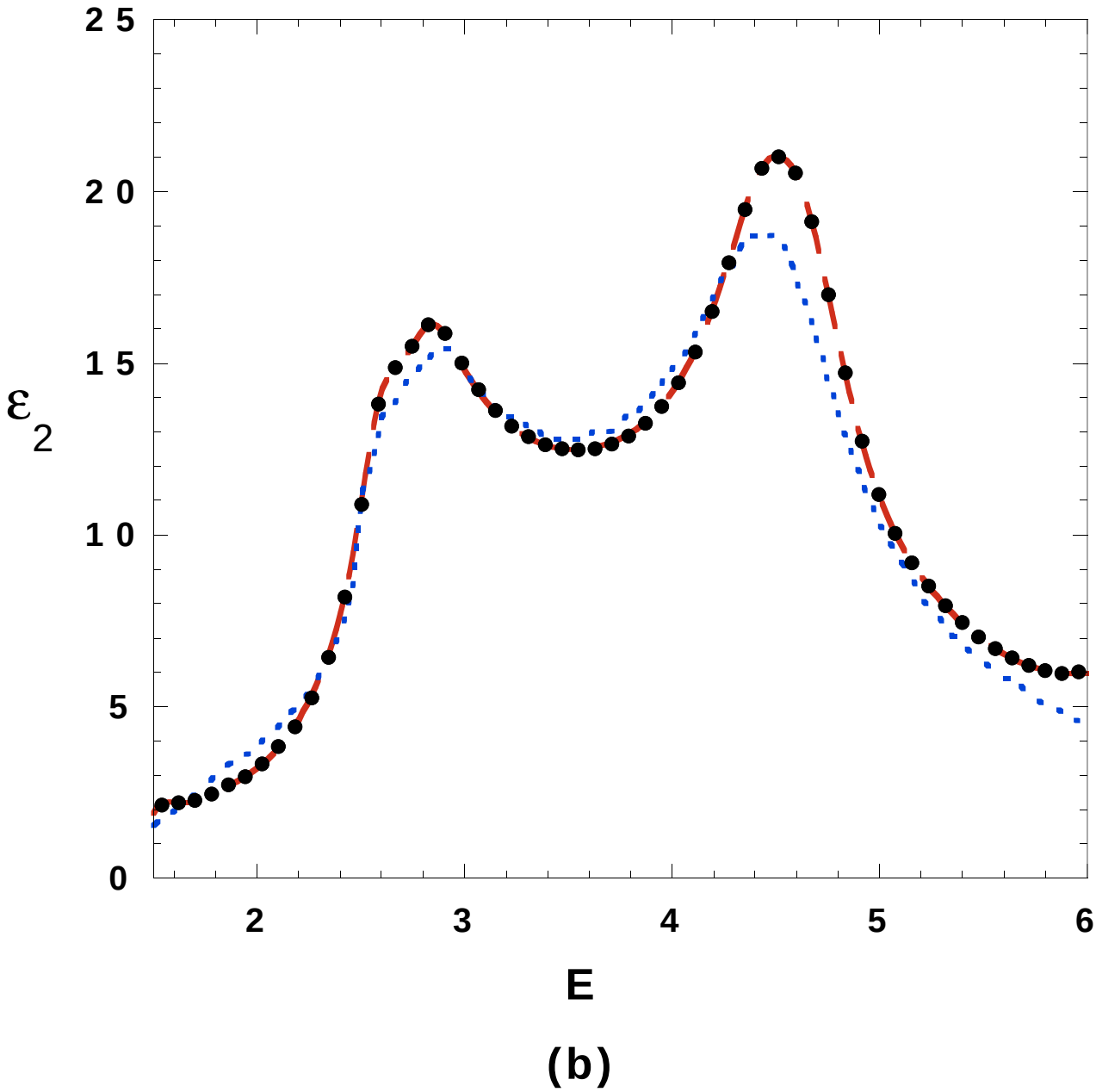

(b)

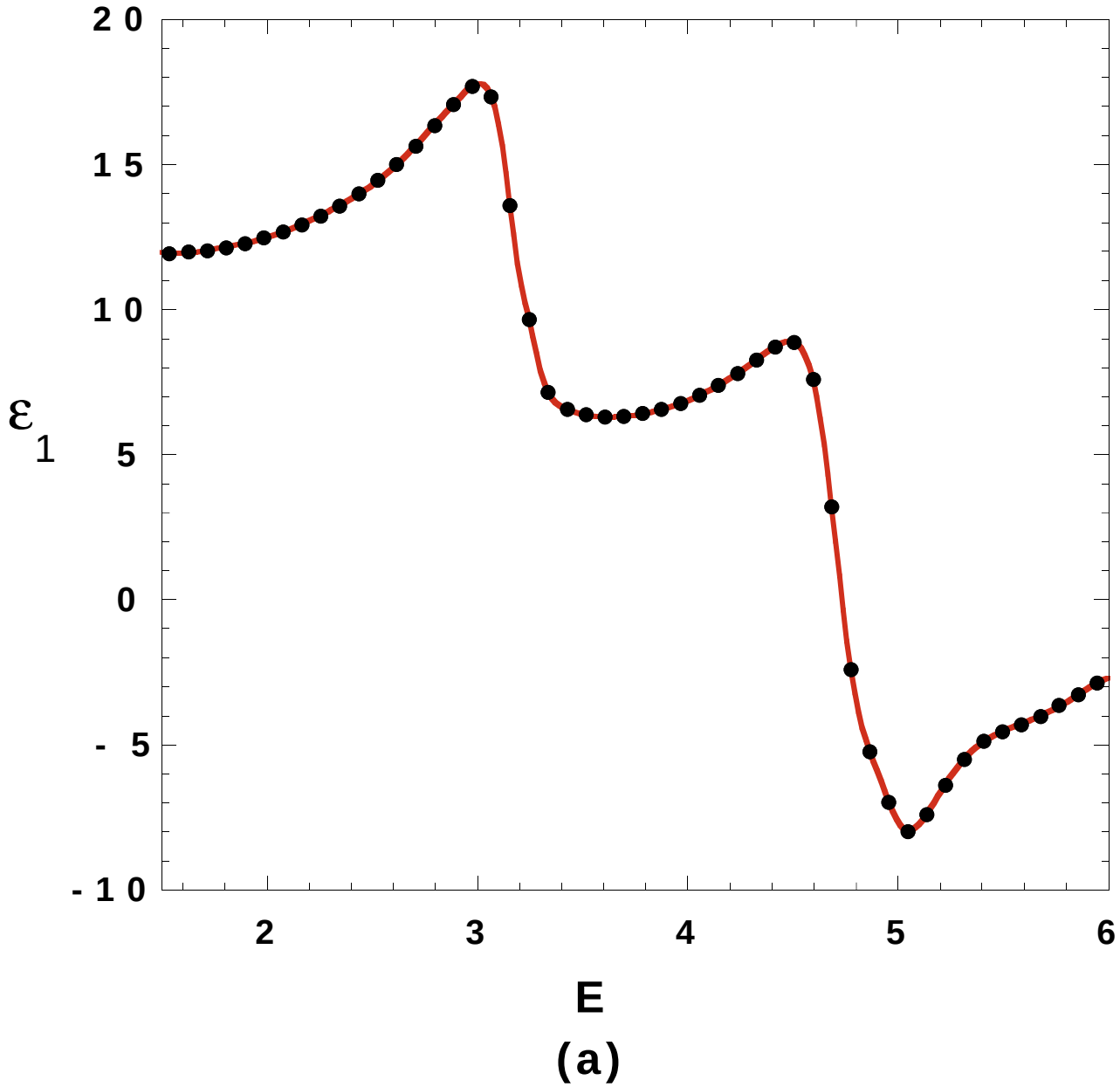

(a)

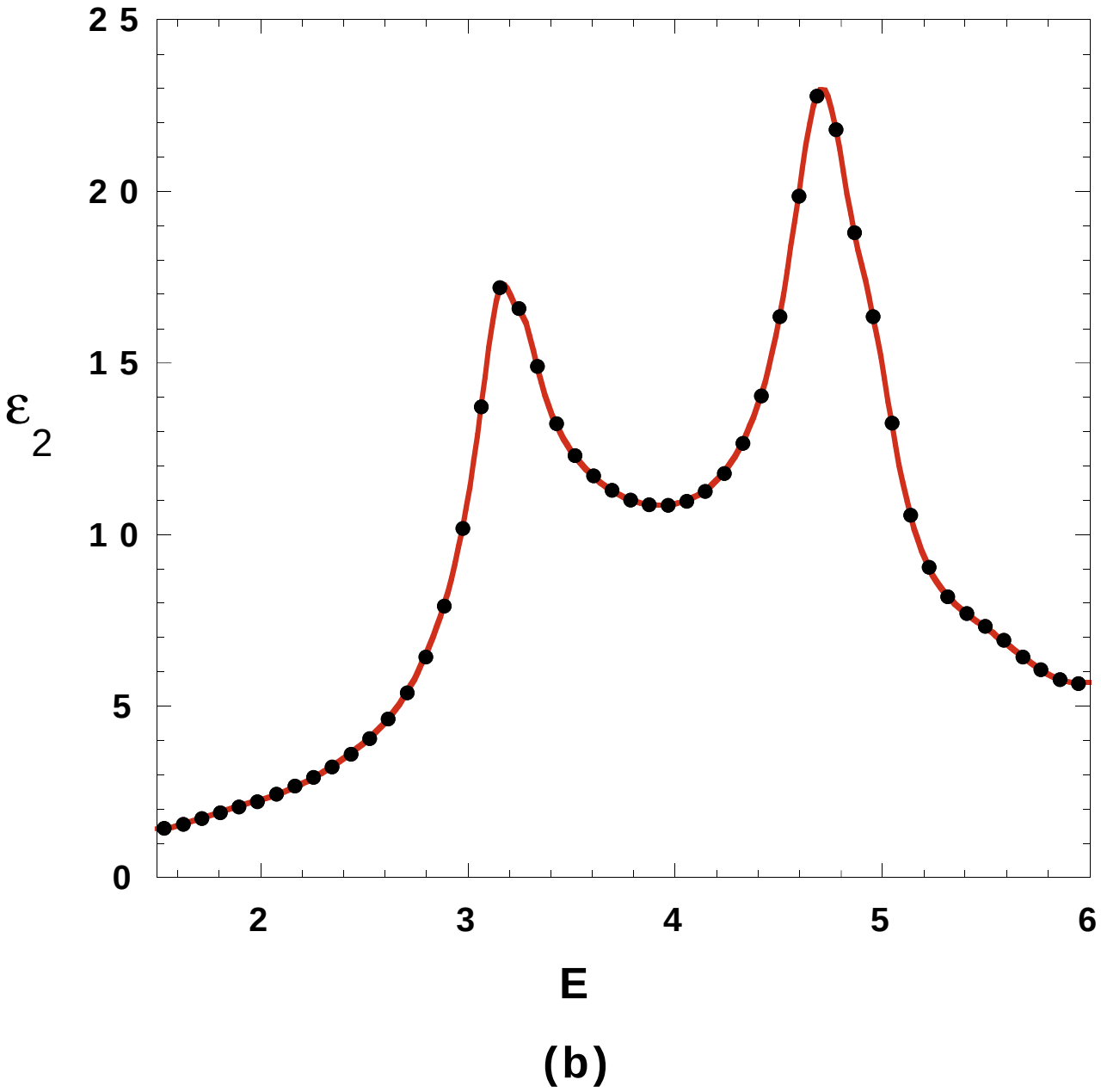
25
20
15
10
5
0
ε2
2
3
4
5
6
E
(b)

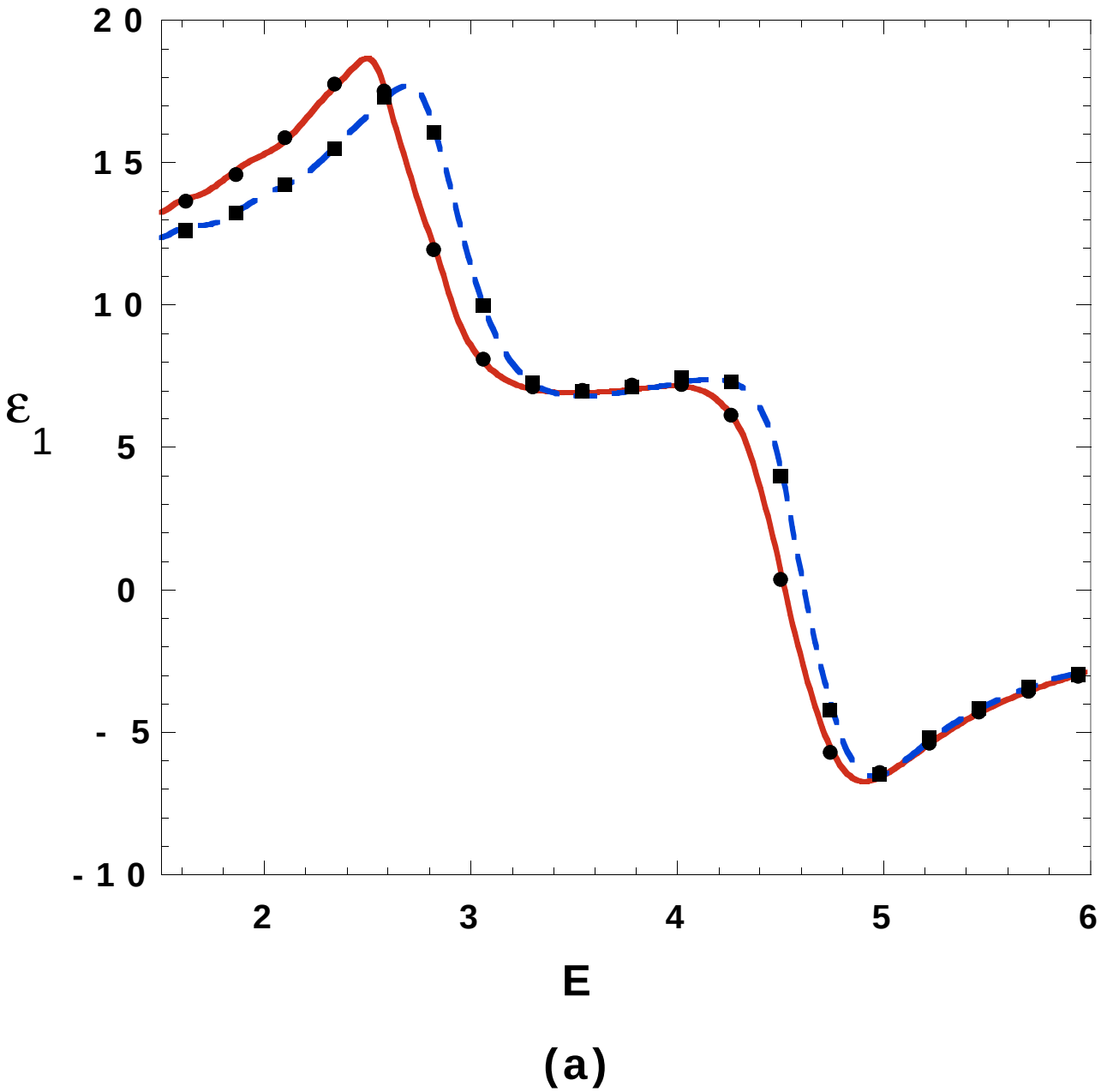

(a)

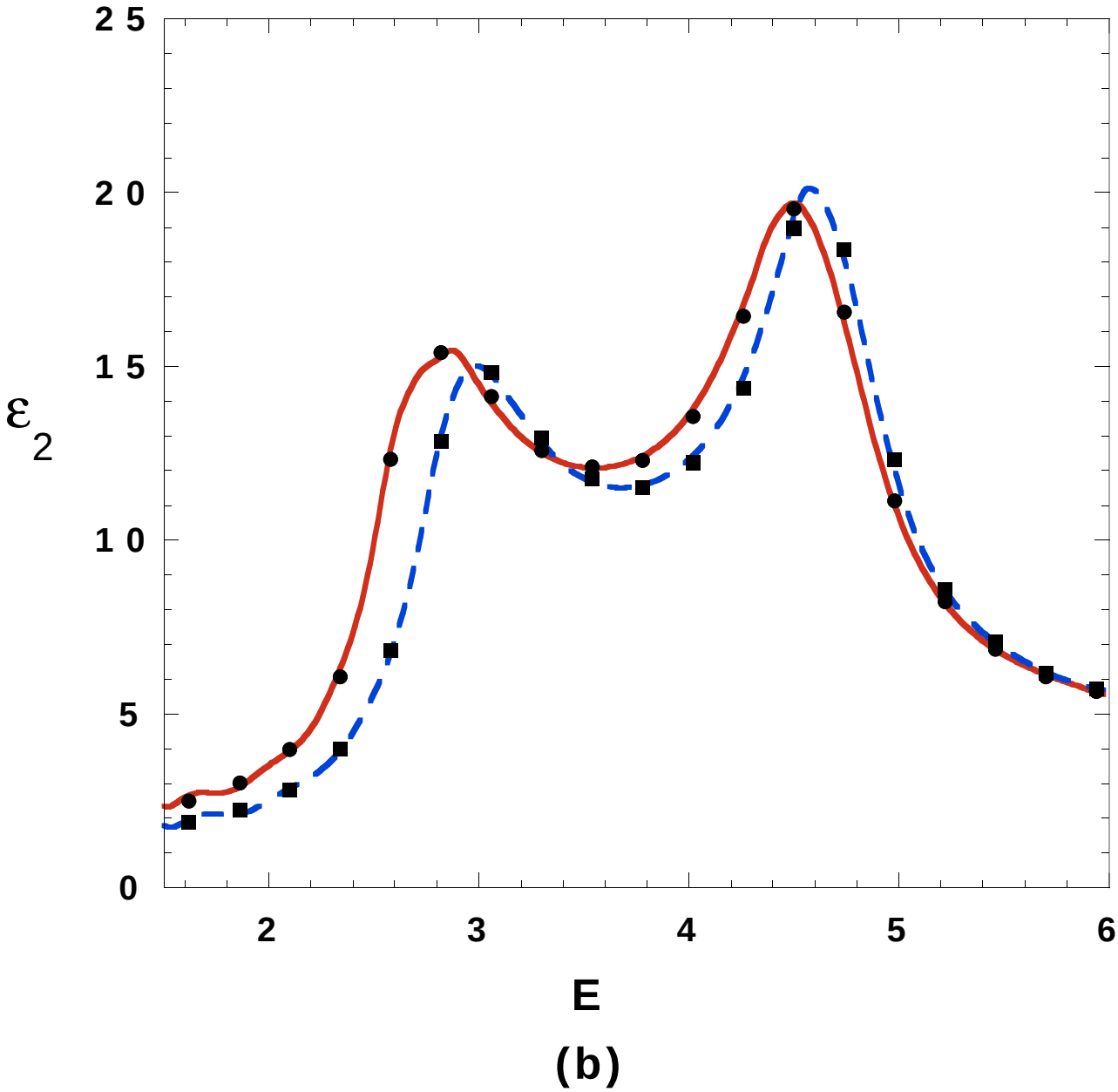
25
20
15
10
5
0
ε2
2
3
4
5
6
E
(b)

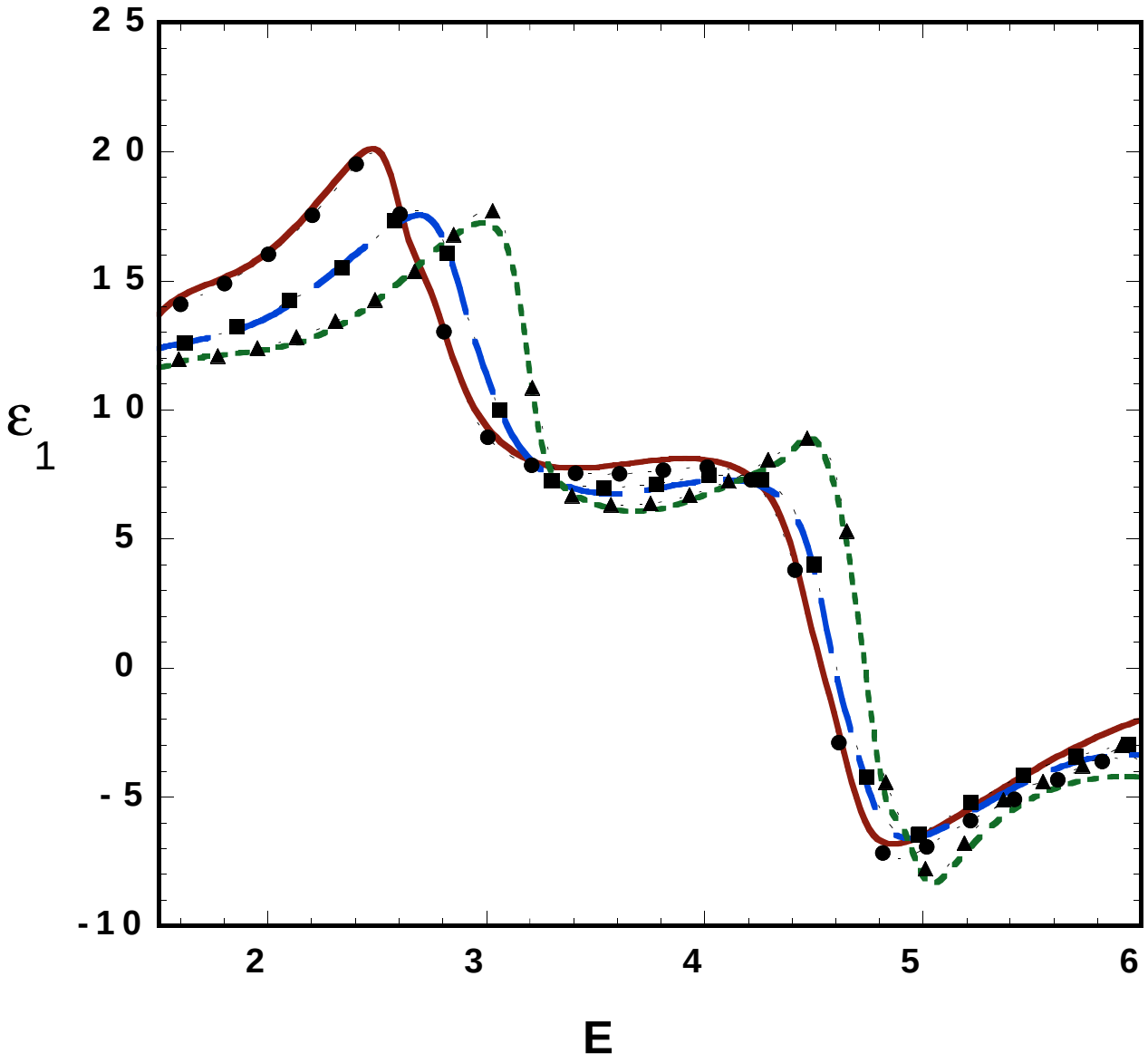
2 5
2 0
1 5
1 0
5
0
- 5
- 1 0
2
3
4
5
6
ε 1
E

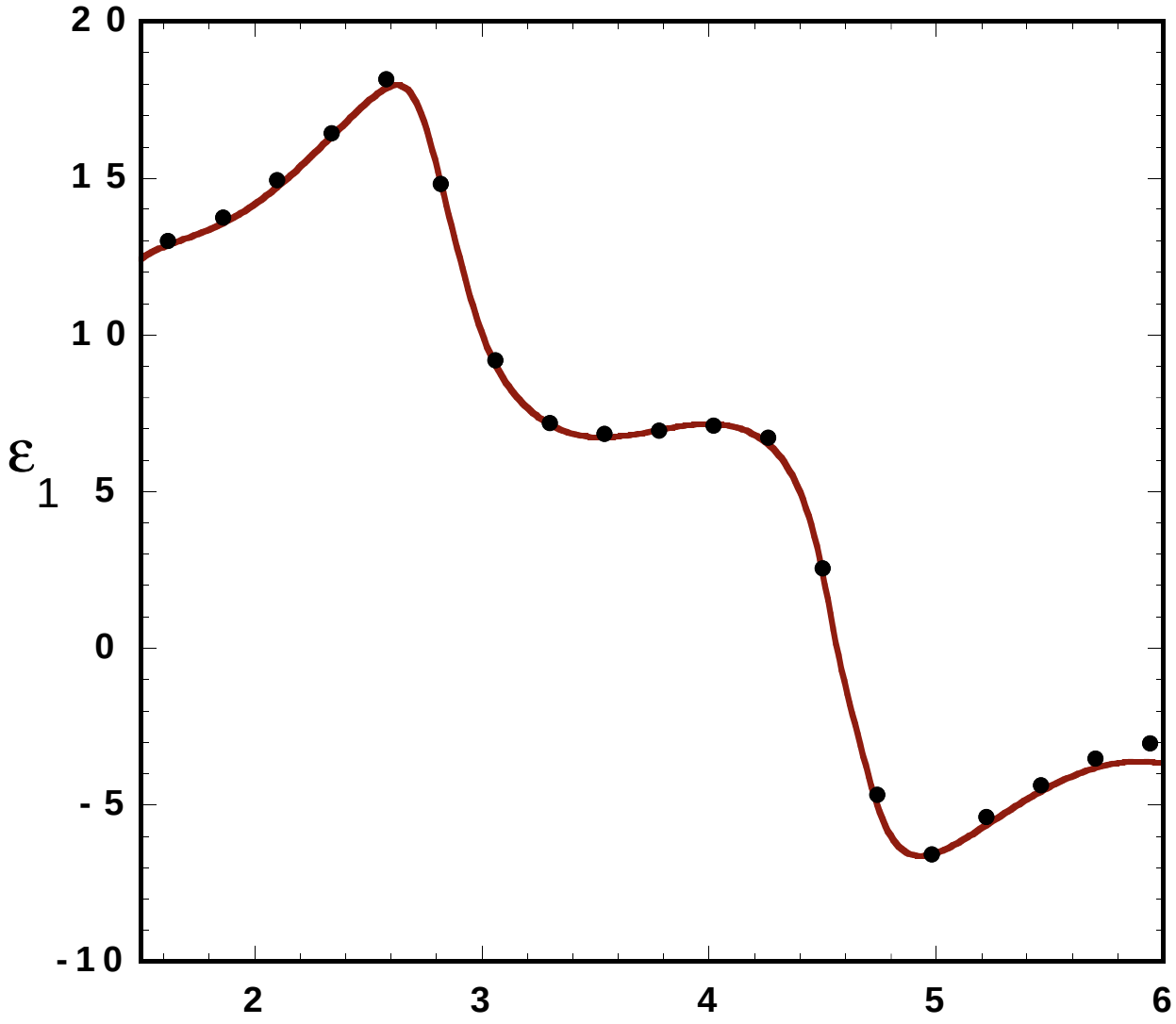

(a)

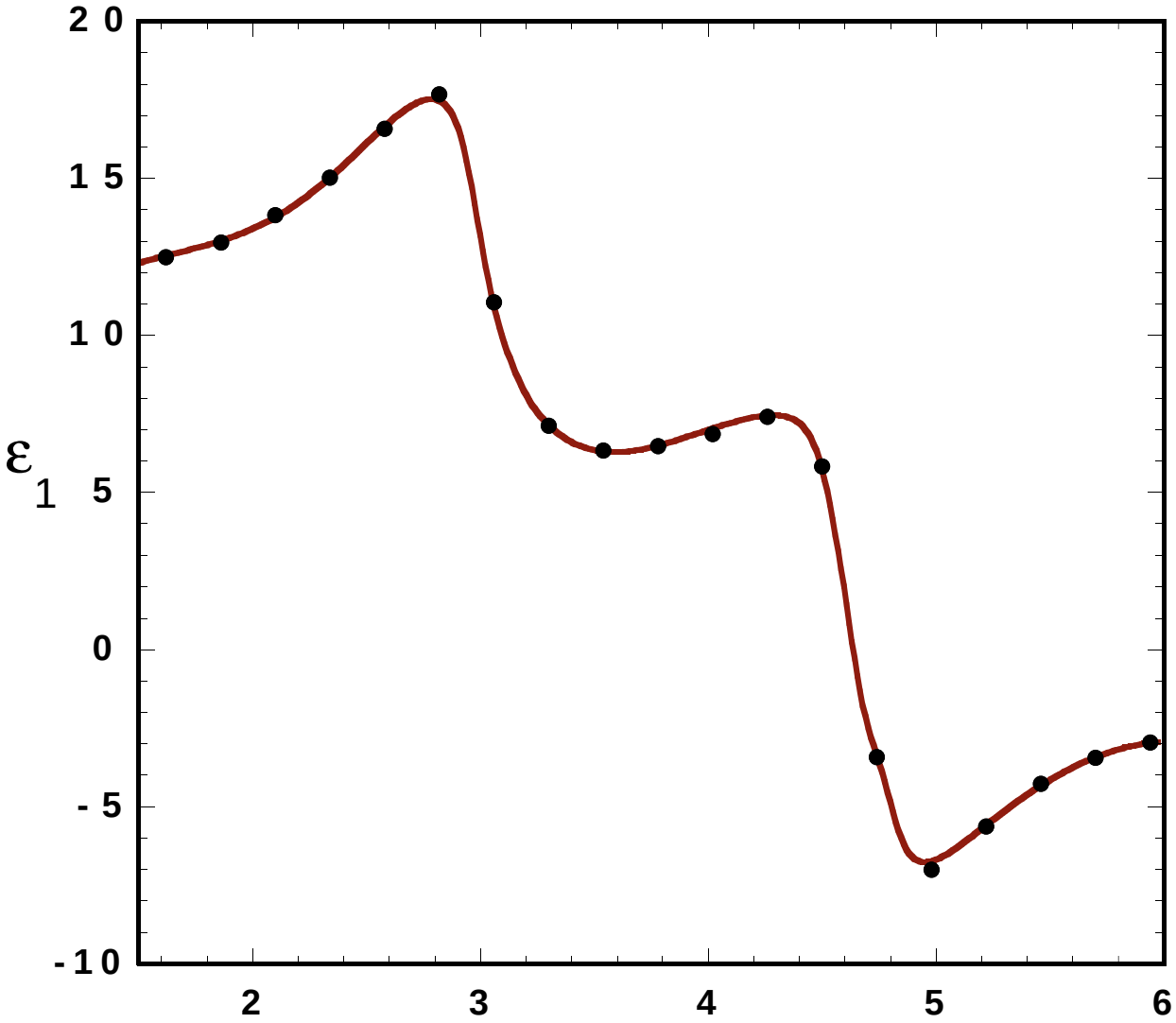

(b)

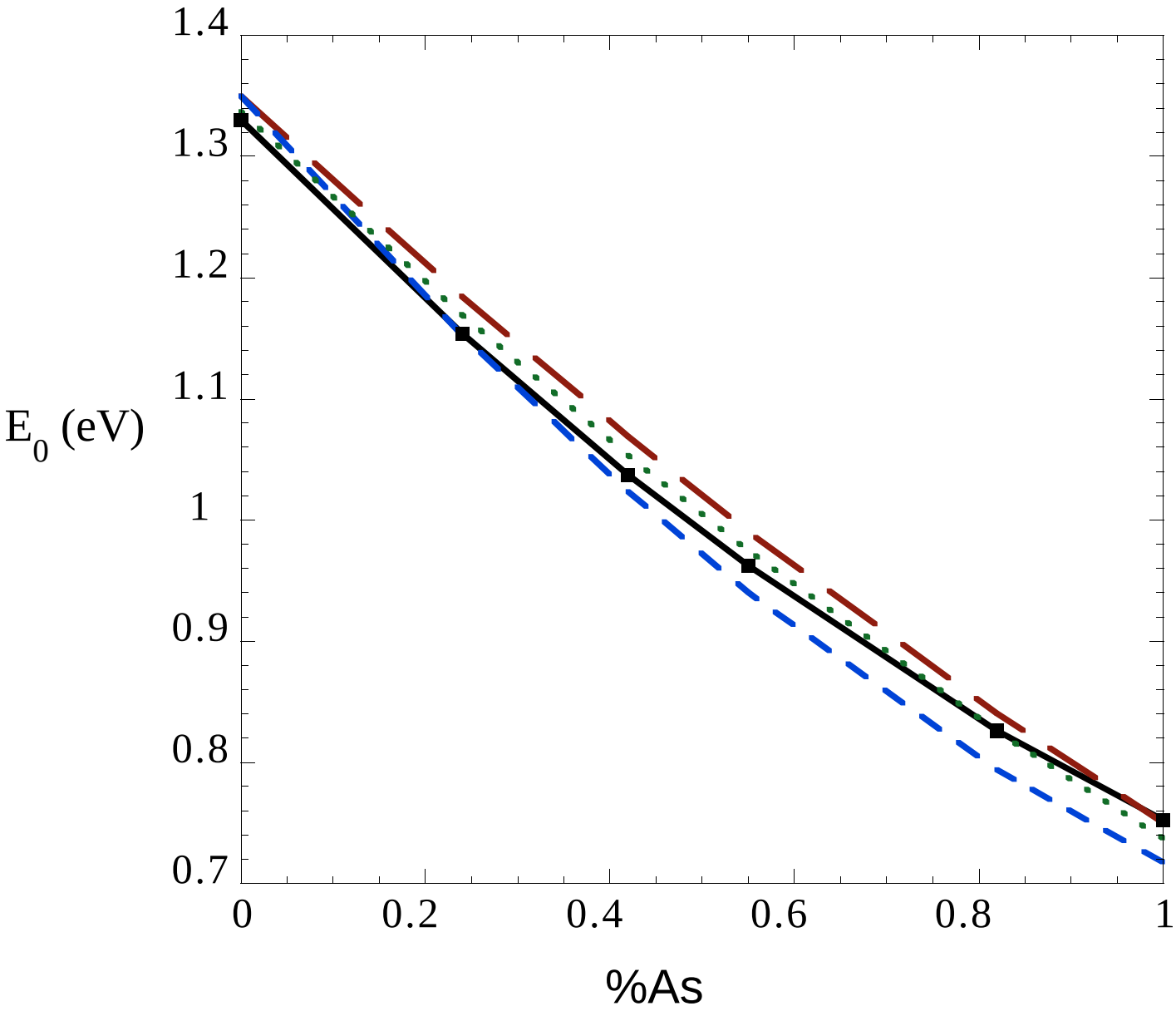
1.4
1.3
1.2
1.1
1
0.9
0.8
0.7
E0 (eV)
0
0.2
0.4
0.6
0.8
1
%As